



THE REAL PART OF THE PROTON – ANTIPROTON ELASTIC SCATTERING AMPLITUDE AT THE CENTRE OF MASS ENERGY OF 546 GEV UA4 Collaboration

Amsterdam¹ – CERN² – Genova³ – Napoli⁴ – Palaiseau⁵ – Pisa⁶

D. Bernard ^{2,*}), M. Bozzo ³), P.L. Braccini ⁶), F. Carbonara ⁴), R. Castaldi ⁶),
F. Cervelli ⁶), G. Chiefari ⁴), E. Drago ⁴), M. Haguenaer ⁵), V. Innocente ^{5,**}), P. Kluit ¹),
S. Lanzano ⁴), G. Matthiae ^{4,***}), L. Merola ⁴), M. Napolitano ⁴), V. Palladino ⁴),
G. Sanguinetti ⁶), P. Scampoli ⁶), S. Scapellato ^{6,†}), G. Sciacca ⁴), G. Sette ³),
J. Timmermans ¹), C. Vannini ⁶), J. Velasco ^{2,††}), P.G. Verdini ⁶) and F. Visco ⁴)

Abstract

Proton–antiproton elastic scattering was measured at the CERN SPS Collider at the centre-of-mass energy $\sqrt{s}=546$ GeV in the Coulomb interference region. The data provide information on the phase of the hadronic amplitude in the forward direction. The conventional analysis gives for the ratio ρ of the real to the imaginary part of the hadronic amplitude the result $\rho = 0.24 \pm 0.04$.

Submitted to Physics Letters B

-
- 1) NIKHEF – H, Amsterdam, The Netherlands
2) CERN, European Organization for Nuclear Research, Geneva, Switzerland
3) Department of Physics and Sezione INFN, Genova, Italy
4) Department of Physics and Sezione INFN, Napoli, Italy
5) Ecole Polytechnique, LPNHE/IN2P3 – CNRS, Palaiseau, France
6) Department of Physics and Sezione INFN, Pisa, Italy

*) Present address: Ecole Polytechnique, Palaiseau, France

**) Present address: Department of Physics and Sezione INFN, Napoli, Italy

***) Present address: University of Rome II, Rome, Italy

†) Present address: Scuola Normale Superiore, Pisa, Italy

††) Present address: IFIC, University of Valencia, Spain

At high-energy and low momentum transfer the amplitude of elastic hadron-hadron scattering is known to be mainly imaginary. The imaginary part of the amplitude is obtained from the total cross section using the optical theorem while the phase is determined experimentally by measuring the interference with the known Coulomb amplitude. Once the real part of the hadronic amplitude is known, the dispersion relations provide a constraint on the behaviour of the total cross section at energies much higher than those accessible to present accelerators.

At the CERN SPS Collider the proton-antiproton total cross section was measured earlier [1] at $\sqrt{s} = 546$ GeV. The experimental result agrees with the prediction of dispersion relations fits on ISR data made a decade ago [2].

In this paper we present a measurement of the real part of the proton-antiproton elastic amplitude at $\sqrt{s} = 546$ GeV. The differential cross section of elastic scattering is given by

$$d\sigma/dt = \pi |f_c + f_h|^2. \quad (1)$$

At low momentum transfer the spin independent hadronic amplitude is usually parametrized in the simple form

$$f_h = (\sigma_{tot}/4\pi) (\rho + i) \exp(-b |t|/2), \quad (2)$$

where ρ is the ratio of the real to the imaginary part. The Coulomb amplitude is $f_c = \pm 2\alpha G^2(t) \exp(\mp i\alpha\phi)/|t|$, where α is the fine structure constant and $G(t)$ is the proton electromagnetic form factor. The Coulomb phase [3] is given by $\phi = \ln(0.08/|t|) - 0.577$. The upper and lower signs refer to $\bar{p}p$ and pp respectively.

At the energy of the SPS Collider the hadronic and the Coulomb amplitudes are equal in magnitude when $|t| \approx 1.1 \cdot 10^{-3}$ GeV². The corresponding scattering angle $\theta \approx 120$ μ rad sets the scale of scattering angles where the relative importance of the interference term between the two amplitudes is maximum. That is the angular region to be studied in order to measure the parameter ρ . It turns out, however, that detection of elastic scattering at these very small angles is not possible at the SPS Collider with a standard high- β scheme as used for our earlier measurement [4] at low momentum transfer ($|t| > 0.03$ GeV²). Since the minimum reachable value of t is proportional to $1/\beta$, a special very high- β configuration was studied and implemented [5]. Only the quadrupoles of the regular SPS lat-

tice were used. A sketch of the layout is shown in Fig.1. A large horizontal β - value was produced at the centre of the horizontally focusing quadrupole QF418 which is in the middle of the long straight section. By a suitable modification of the strength of the neighbouring quadrupoles, values of β_h as high as 1000 m are obtained, while β_v is hardly changed and the appropriate matching of the insertion to the rest of the SPS lattice is achieved. The crossing region of the proton and antiproton bunches which, in the normal Collider operation is mid - way between the quadrupoles QF418 and QD419 was displaced inside the quadrupole QF418. Also shown in Fig.1 is a plot of the β functions in the horizontal and vertical plane. At the crossing point, $\beta_h = 1086$ m and $\beta_v = 22$ m.

Elastic events were detected in the horizontal plane by a system of telescopes located close to the nearest minimum of β_h and placed in the machine plane symmetrically on both sides of the vacuum pipe. Each telescope of the left side (incoming protons side) consists of two Roman pots, 0.6 m apart, at a distance of 43 m from the crossing. The telescopes on the right side (incoming antiprotons side) consist of a single Roman pot at a distance of 94 m from the crossing. On this side no space was available in the machine structure for a second detector. Each Roman pot contains a trigger counter, a hodoscope with eight horizontal scintillator counters and a chamber with wires in the vertical direction. The chamber has four drift planes for the measurement of the horizontal coordinate and a proportional plane measuring the vertical coordinate by the charge division method. Detailed information on the Roman pots and on the detectors can be found in ref.[6].

The particles scattered in the crossing region traverse quadrupoles of the machine lattice (on the right side also a bending section) before reaching the detectors. Particle trajectories were calculated using the standard formalism of the transfer matrices. The "effective distances" of the detectors from the crossing point in the horizontal and vertical plane were $L_h = 58$ m and $L_v = 27.5$ m on the left side and $L_h = 127$ m and $L_v = 15.7$ m on the right side.

The present experiment was performed during a dedicated run of a few days of the SPS Collider. The basic requirement being the detection of very small angle scattering events, considerable effort was put to obtain clean beams. The collimators in the machine were set to cut the beam tails beyond four standard deviations of the beam size. Additional scraping was then performed during data taking to remove the tails which were slowly building up. The Roman pots were set such that the inner edge of

the detectors was at ≈ 8 mm from the beam axis in the left side and ≈ 12 mm in the right side, corresponding to a minimum scattering angle of $140 \mu\text{rad}$ ($|t| = 1.5 \cdot 10^{-3} \text{ GeV}^2$). With this setting the background was rather high but tolerable. Data taking was distributed in six different stacks with average luminosity around $2 \cdot 10^{26} \text{ cm}^{-2} \text{ s}^{-1}$. The trigger rate was $5 - 10$ Hz. A total of ≈ 850 K triggers were collected.

Position and emittance of the beams were regularly measured during data taking by means of the beam position monitors and of the wire scan system [7]. Typical r.m.s. values of the transverse dimensions of the proton bunches at the crossing were 4.6 mm and 0.7 mm in the horizontal and vertical plane, respectively. The angular spread was $4.3 \mu\text{rad}$ horizontally and $30 \mu\text{rad}$ vertically. The corresponding figures for the antiproton bunches were $\approx 20\%$ smaller. The large size and small angular spread of the beam in the horizontal plane are a consequence of the very large value of β_H . The longitudinal distribution of the crossing region had a r.m.s. value of 18 cm.

The analysis of the data was performed in the following way.

1) Calibration parameters and detection efficiencies of the chambers were obtained from a sample of preselected elastic events. The measured resolution on the horizontal coordinate was $\approx 130 \mu\text{m}$ per drift plane and did not show any sizeable deterioration near the inner edge of the chambers. The charge division parameters of the proportional plane were obtained by comparison to the distribution of hits in the hodoscope counters. The resolution on the vertical coordinate as given by the charge division was normally of ≈ 0.4 mm. Due to the large value of the local background close to the edge of the pots on the left side, this resolution was there a factor of two worse.

The detection efficiency of each chamber plane was studied as a function of the horizontal coordinate. A reduction of efficiency was observed in some planes near the inner edge of the chambers and around the sense wires. Track reconstruction was performed by demanding at least 4 drift planes out of 8 in the telescopes on the left side (P1*P3 and P2*P4) and 2 out of 4 in those on the right side (P5 and P6). In addition, one hit was required in the proportional planes on each side. These criteria ensured an overall efficiency close to one over the full sensitive area of the detectors, as a consequence of the redundancy in the number of detector planes.

2) After track reconstruction and application of standard rejection criteria involving number of tracks per telescope, the following selections were made.

- Cut on the horizontal coordinate $x_0(\bar{p})$ of the antiproton trajectory at the centre of the crossing region. The lever arm for the telescopes of the left side (outgoing antiprotons) is such that this quantity could be determined with an error of ≈ 1 cm. A similar selection could not be made on the right side where only one pot per telescope was available.
- Cut on the left-right collinearity distribution in the vertical plane, i.e. on the quantity $\Delta\theta_v = y(\bar{p})/L_v(\bar{p}) - y(p)/L_v(p)$.
- Cut on the left-right collinearity distribution in the horizontal plane i.e. on the quantity $\Delta\theta_h = x(\bar{p})/L_h(\bar{p}) - x(p)/L_h(p)$.

These cuts were made at the 3.5 standard deviations level. After all selections a sample of $\approx 100K$ events was left. Distributions of the quantities $\Delta\theta_v$ and $\Delta\theta_h$ are presented in Fig.2. The collinearity distributions have r.m.s. value of $\approx 8 \mu\text{rad}$ horizontally and $\approx 55 \mu\text{rad}$ vertically. These figures agree well with the expectations from the direct measurements of the beam profile.

The transverse position of the beam was determined from the distribution of the intercept at the crossing point of the reconstructed line between the measured points on the p and \bar{p} side. The beam displacement is reflected in the off-set of the $\Delta\theta_v$ and $\Delta\theta_h$ distributions and turned out to be 6 mm horizontally and 1.6 mm vertically. These results were consistent with the information provided by the beam position monitors. The longitudinal position of the crossing region was obtained, with an error of ≈ 3 cm, from time-of-flight measurements by the trigger counters of incoming and outgoing tracks on both the left and right sides.

3) A complete Monte-Carlo simulation of the experiment was performed including both the beam parameters (position, size, angular spread) and the detector parameters (resolution and efficiency of the individual chamber planes). The results of the Monte-Carlo were used to obtain the t -distribution, corrected for the geometrical acceptance, for the detector efficiency and for the experimental t -resolution.

Fiducial cuts were applied in the θ_h, θ_v plane in order to select a safe region of acceptance within the area of the detectors and inside the machine vacuum chambers. The interval of momentum transfer where the acceptance can be trusted with confidence ranges from $|t|_{\min} = 0.002 \text{ GeV}^2$ ($\theta = 165 \mu\text{rad}$) up to $|t|_{\max} = 0.035 \text{ GeV}^2$. The final number of elastic events in this interval is 70 K. The momentum transfer resolution is essentially determined by the angular spread of the beams and is given by $\Delta t = a\sqrt{|t|}$ where a varies from 0.01 at $t = t_{\min}$ up to 0.02 at $t = t_{\max}$.

4) In order to reconstruct the actual value of the scattering angle, one has to know the angle of the beam with respect to the nominal machine axis. The beam angle in the vertical plane α_v was inferred from the observed up-down asymmetry of the track distribution with respect to the machine plane. It was found $\alpha_v = 90 \pm 10 \mu\text{rad}$, a value that has a relatively small effect on the determination of the scattering angle. The horizontal beam angle α_h was obtained as in our earlier measurement of elastic scattering [4], by comparing the two samples of elastic events resulting from the two detection arms (P1*P2*P5 and P3*P4*P6). It was found to be $\alpha_h = 11 \pm 8 \mu\text{rad}$. The actual scattering angle for each individual event was obtained by combining the information from the left and right side telescopes and correcting for the measured values of α_h and α_v . The same correction was also included in the Monte-Carlo simulation in order to obtain the t -distribution dN/dt as a function of t . The background which is present under the elastic peak of Fig.2b within the cuts was estimated from the tails of the distribution and then subtracted. The correction is $\approx 0.5\%$ on the average, rising to 1.5% at very low $-t$.

5) The last step in the analysis consists of fitting the data to the theoretical form of the differential cross section using the relation $dN/dt = \mathcal{L} d\sigma/dt$, where $d\sigma/dt$ is given by eq. (1) and \mathcal{L} is the unknown machine luminosity integrated over the data taking period. In our earlier measurement of the proton-antiproton total cross section [1], the combination $\sigma_{\text{tot}}(1 + \rho^2)$ was measured. The result was $\sigma_{\text{tot}}(1 + \rho^2) = 63.3 \pm 1.5 \text{ mb}$. This information was always used in the analysis of the present data in order to fix the absolute normalization.

A fit was first performed in the full t -range ($0.002 < |t| < 0.035 \text{ GeV}^2$) leaving b and ρ as free parameters, in addition to \mathcal{L} . The result of this fit was $b = 15.5 \pm 0.8 \text{ GeV}^{-2}$ and $\rho = 0.23 \pm 0.04$, the quoted errors being statistical. Leaving out the first data points, the correlation between b and ρ is

greatly reduced. A fit in the interval $0.006 < |t| < 0.035 \text{ GeV}^2$ with ρ fixed to the value 0.23, again gave $b = 15.5 \pm 0.7 \text{ GeV}^{-2}$. The value of the parameter b as obtained from these fits agrees well with the result $b = 15.3 \pm 0.3 \text{ GeV}^{-2}$ found in our earlier measurement of elastic scattering in the momentum transfer range $0.03 < |t| < 0.10 \text{ GeV}^2$ [4]. This earlier, more accurate result was then used as fixed parameter in our final fit while ρ and \mathcal{L} were left as free parameters. The result of the final fit is $\rho = 0.238 \pm 0.024$, the quoted error being statistical. The measured differential cross sections are shown in Fig.3a and also listed in Table 1. The absolute normalization is fixed by the value of the parameter \mathcal{L} as determined from the fit. The result of the fit is also shown in Fig.3a together with the individual contributions of the Coulomb and hadronic terms. The ratio $R(t) = (d\sigma/dt)_{\text{meas}} / (d\sigma/dt)_{\rho=0} - 1$ which shows the effect of the interference term in the data is plotted in Fig.3b.

The measurement of ρ is affected by various systematic uncertainties. The correlation between ρ , σ_{tot} and b is given numerically by $\partial\rho/\partial\sigma_{\text{tot}} = 0.009 \text{ mb}^{-1}$ and $\partial\rho/\partial b = -0.04 \text{ GeV}^2$. The error on ρ which is induced by the errors on the measurements of σ_{tot} and b is then $\Delta\rho \approx 0.02$. The uncertainty on the relative position of the pots ($100 \mu\text{m}$) gives $\Delta\rho \approx 0.015$. Other sources of error are expected to give negligible contributions. A quadratic combination of the errors mentioned above gives $\Delta\rho_{\text{syst}} \approx 0.025$. As a final result of our measurement we then quote $\rho = 0.24 \pm 0.04$. Our data point is shown in Fig.4 together with a compilation [8] of results on pp and $\bar{p}p$ scattering at lower energies. Note that with this measured value of ρ , our result on the total cross section [1] should be rescaled to $\sigma_{\text{tot}} = 60 \pm 2 \text{ mb}$.

The present result was derived using the conventional parametrization of the hadronic amplitude as given by eq.(2), with a constant slope b and a constant ratio of the real to the imaginary part. However, recent models of high-energy scattering [9] predict that the logarithmic slope of the differential cross section may change appreciably even in the small t -range covered by the present experiment. In addition, the real part of the hadronic amplitude may decrease with t faster than the imaginary part. The sensitivity of the parameter ρ to these effects was studied and found to be small but not negligible. In fact,

- If the real and the imaginary part have the same t -dependence, but the slope parameter b is changing with t , being equal to 15.3 GeV^{-2} at $|t|=0.06 \text{ GeV}^2$, to 15.7 GeV^{-2} at $|t|=0.04 \text{ GeV}^2$, raising to 17.2 GeV^{-2} at $|t|=0$, then ρ should be lowered by 0.02.
- If the slope of the real part is twice as large as that of the imaginary part, then ρ should be lowered by 0.03.

The result of our measurement of ρ is definitely higher than the range of values anticipated by the current fits to data on σ_{tot} and ρ using either dispersion relations or parametrizations with suitable analytical functions of the scattering amplitude [2,10]. When the energy dependence of the total cross section is parametrized with a leading term proportional to $(\ln s)^2$, the predicted value of ρ at the SPS Collider is $\rho \approx 0.15$. If the total cross section is assumed to flatten off in a significant way at energies of a few TeV, smaller values of ρ are predicted, around 0.1.

Therefore, the present result strongly favours a fast rise of the total cross section with energy, suggesting in fact that the local rise of the total cross section in the energy region around $\sqrt{s} = 1 \text{ TeV}$ might be larger than it was anticipated.

A less conventional, alternative interpretation is however offered by the hypothesis that the odd-under-crossing amplitude is not negligible [11]. In that case, the pp and $\bar{p}p$ total cross sections would be different at very high energy.

We wish to thank A. Martin for his continuous interest in this experiment and for several enlightening discussions. We are very grateful to P.E. Faucher, A. Faugier and A. Hilaire for the study and actual implementation of the special high- β scheme that was requested to perform the present experiment. We wish also to express our gratitude to the overall staff of the CERN Accelerator Divisions for the successful operation of the SPS Collider during the dedicated run which was devoted to this experiment. The assistance of our technicians at CERN, INFN and NIKHEF is also warmly acknowledged.

REFERENCES

- [1] UA4 Collaboration, M. Bozzo et al., Phys. Lett. 147B (1984) 392.
- [2] U. Amaldi et al., Phys. Lett. 66B (1977) 390.
- [3] R. Cahn, Zeitschr. für Phys. C15 (1982) 253.
- [4] UA4 Collaboration, M. Bozzo et al., Phys. Lett. 147B (1984) 385.
- [5] P.E. Faugeras, CERN Internal note, CERN/SPS 84-7 (ARF), 1984;
P.E. Faugeras et al., CERN Internal note, CERN/SPS/DI-MST/ME 85-03 (1985)
- [6] J. Buskens et al., Nucl. Instrum. and Met. 207 (1983) 365;
R. Battiston et al., Nucl. Instrum. and Meth. A238 (1985) 35.
- [7] J. Bossler et al., Nucl. Instrum. and Meth. A235 (1985) 475.
- [8] N. Amos et al., Nucl. Phys. B262 (1985) 689.
- [9] C. Bourrely et al., Nucl. Phys. B247 (1984) 15;
R.J. Glauber and J. Velasco, Phys. Lett. 147B (1984) 380;
R. Henzi and P. Valin, Phys. Lett. 149B (1984) 239.
- [10] A. Martin, Proceedings of the Workshop on $p\bar{p}$ Collider Physics, Bern (1984) 308;
M. Block and R.N. Cahn, Phys. Lett. B188 (1987) 143.
- [11] K. Kang and B. Nicolescu, Phys. Rev. D11 (1975) 2461;
A. Donnachie and P.V. Landshoff, Nucl. Phys. B231 (1984) 189;
B. Nicolescu, Proceedings of the 7th European Symposium on Antiproton Interactions,
Durham, UK (1984) 411.

Table 1:

$ t $ (GeV ²) ($\times 10^{-3}$)	$d\sigma/dt$ (mb/GeV ²)	Error	$ t $ (GeV ²) ($\times 10^{-3}$)	$d\sigma/dt$ (mb/GeV ²)	Error	$ t $ (GeV ²) ($\times 10^{-3}$)	$d\sigma/dt$ (mb/GeV ²)	Error
2.25	265.	8.	13.25	163.	4.	24.25	131.	5.
2.75	246.	7.	13.75	151.	4.	24.75	135.	5.
3.25	248.	6.	14.25	157.	4.	25.25	130.	5.
3.75	215.	6.	14.75	167.	4.	25.75	131.	5.
4.25	218.	5.	15.25	157.	4.	26.25	134.	6.
4.75	216.	5.	15.75	159.	4.	26.75	121.	5.
5.25	208.	5.	16.25	159.	4.	27.25	139.	6.
5.75	209.	5.	16.75	160.	4.	27.75	135.	6.
6.25	198.	5.	17.25	154.	4.	28.25	119.	5.
6.75	199.	5.	17.75	152.	4.	28.75	126.	6.
7.25	189.	4.	18.25	158.	5.	29.25	132.	6.
7.75	188.	4.	18.75	151.	5.	29.75	125.	6.
8.25	188.	4.	19.25	150.	5.	30.25	126.	6.
8.75	188.	4.	19.75	151.	5.	30.75	132.	6.
9.25	188.	4.	20.25	140.	5.	31.25	135.	7.
9.75	182.	4.	20.75	143.	5.	31.75	132.	7.
10.25	184.	4.	21.25	133.	5.	32.25	128.	7.
10.75	170.	4.	21.75	148.	5.	32.75	119.	7.
11.25	168.	4.	22.25	135.	5.	33.25	118.	7.
11.75	168.	4.	22.75	149.	5.	33.75	111.	7.
12.25	165.	4.	23.25	143.	5.	34.25	115.	8.
12.75	162.	4.	23.75	144.	5.	34.75	118.	8.

FIGURE CAPTIONS

- Fig. 1 Layout of the experiment on elastic scattering in the Coulomb interference region at the CERN SPS Collider. The machine quadrupoles QF (horizontally focussing) and QD (horizontally defocussing), the bending magnets M and the Roman pots, P1 to P6 are shown in a top view together with the behaviour of the betatron functions.
- Fig. 2 (a) Collinearity distribution in the vertical plane.
(b) Collinearity distribution in the horizontal plane.
The arrows indicate the position of the cuts.
- Fig. 3 (a) The measured differential cross section as a function of t . The bin width is $5 \cdot 10^{-4} \text{ GeV}^2$.
The solid line represents the best fit. Also shown the contribution of the different terms.
(b) The ratio $R(t)$ as defined in the text.
- Fig. 4 The present result on the parameter ρ is shown together with lower energy data for pp and $\bar{p}p$ elastic scattering.

The high- β insertion for Coulomb scattering at the CERN collider

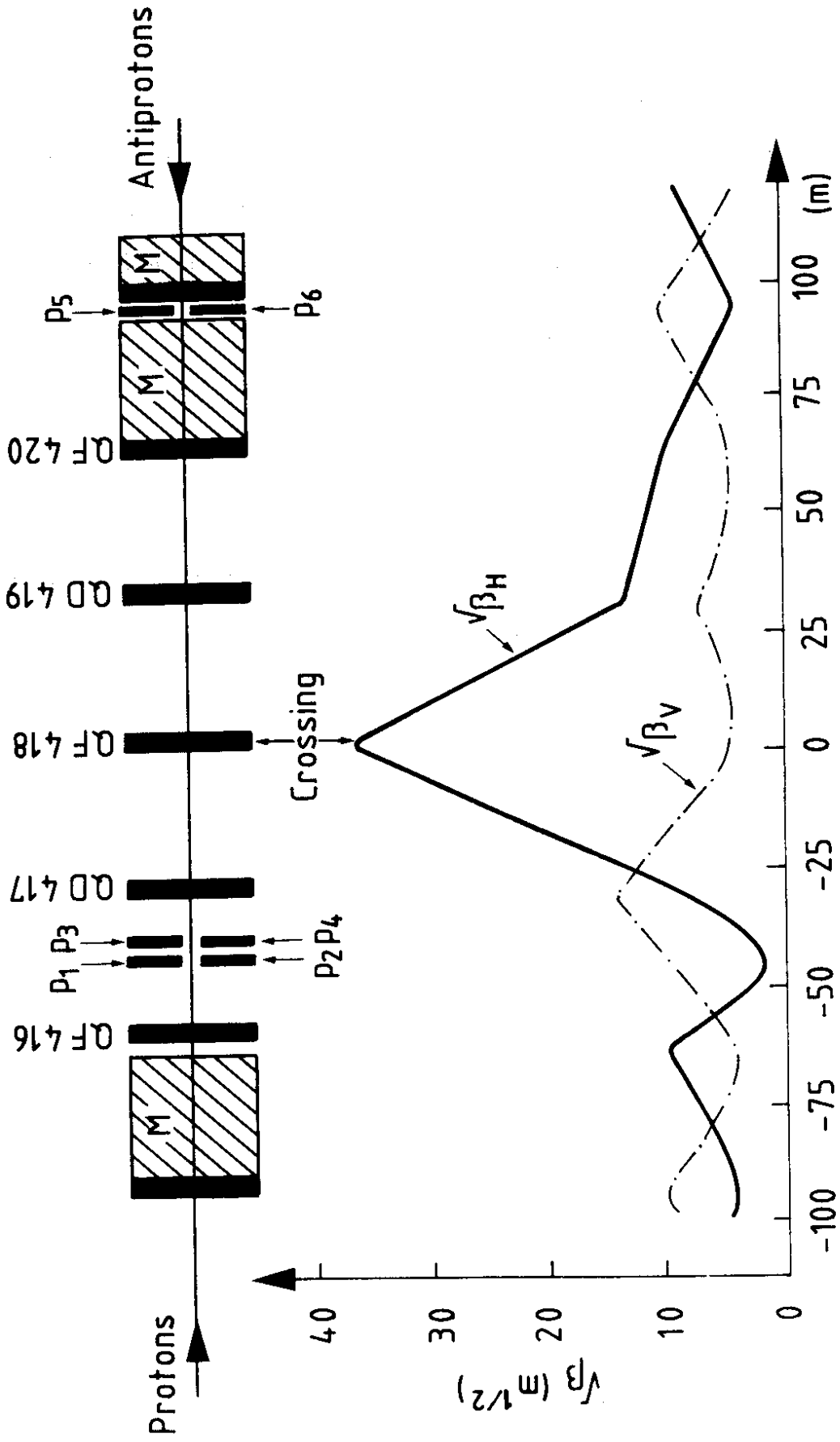


Fig. 1

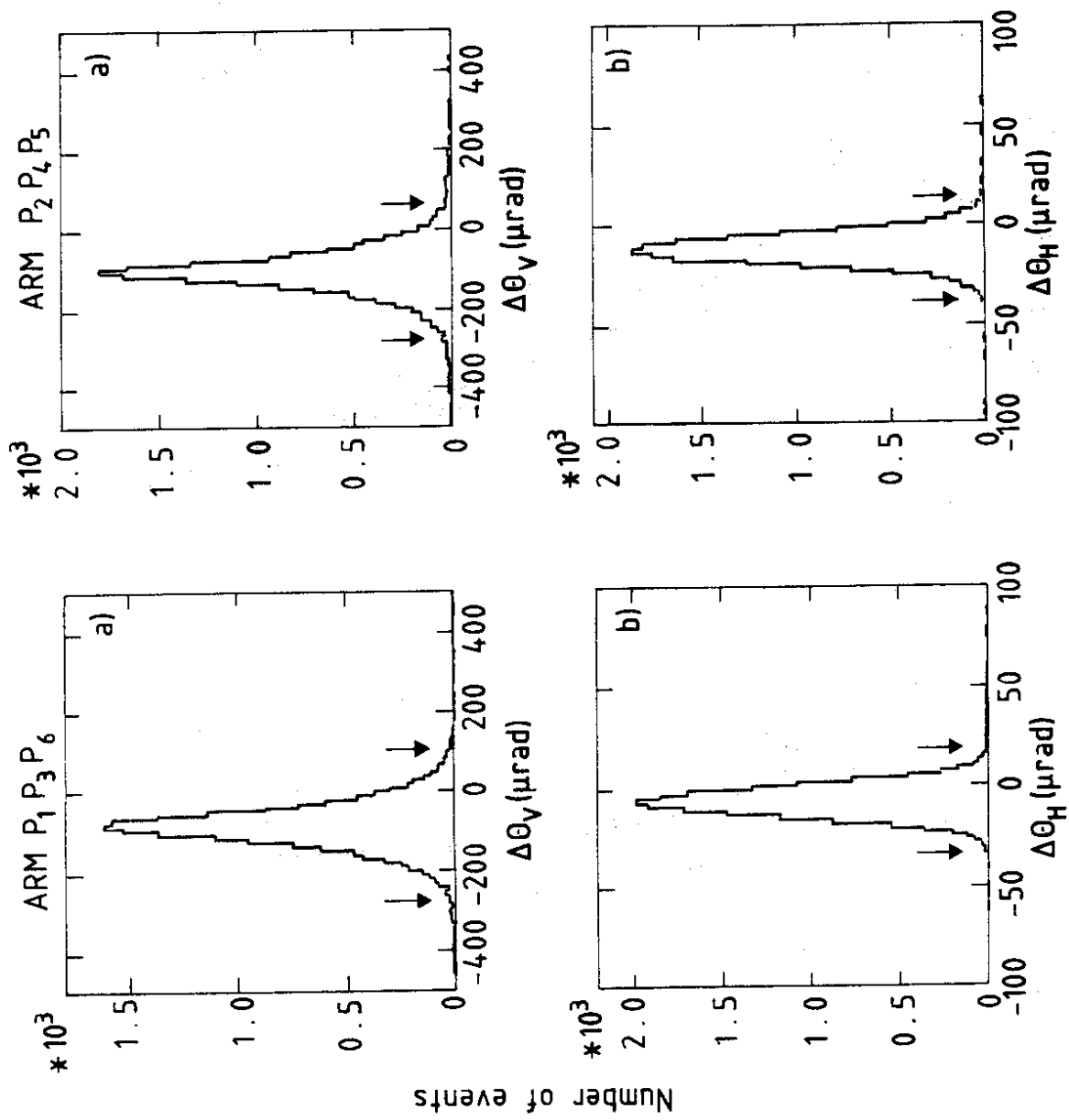


Fig. 2

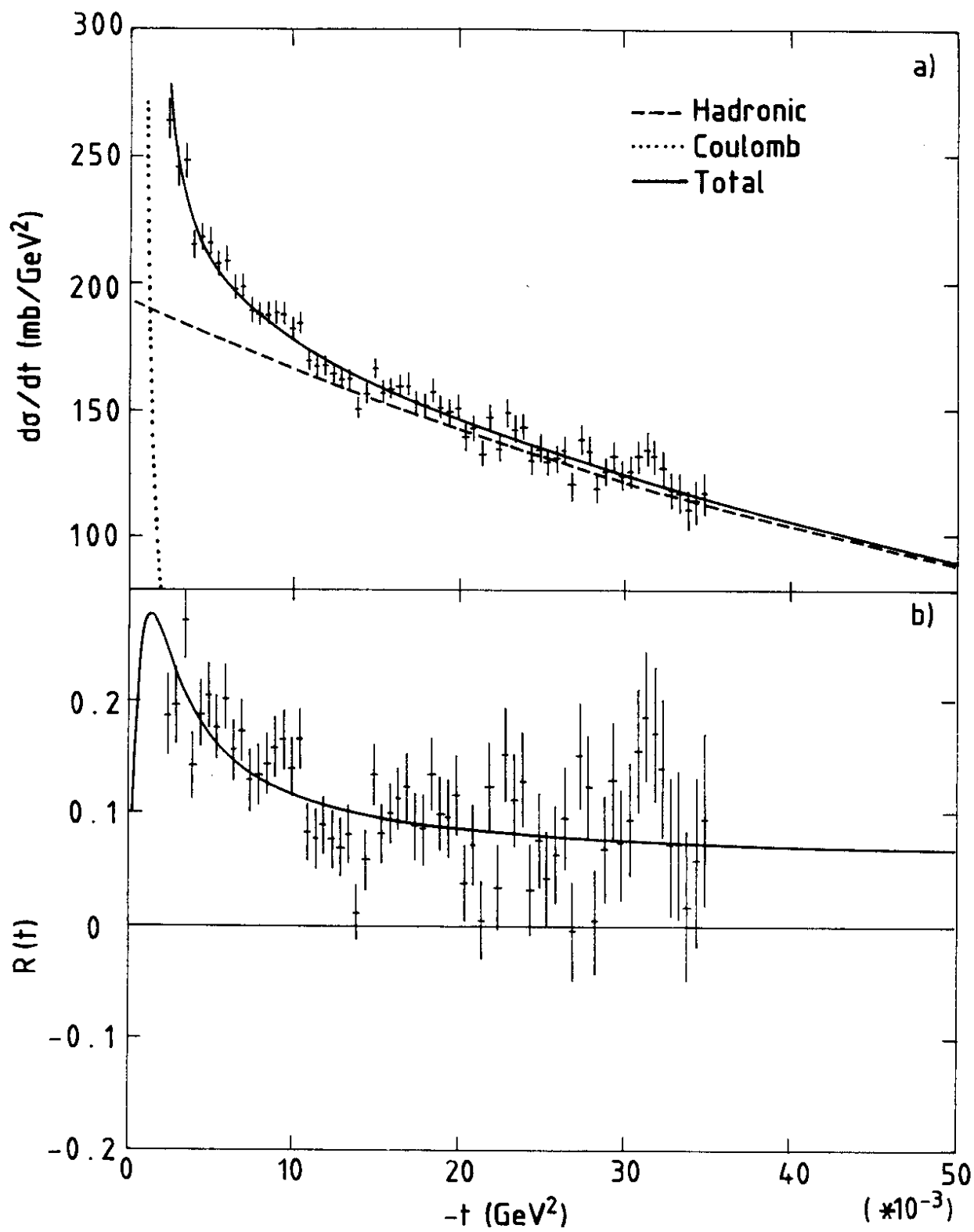


Fig. 3

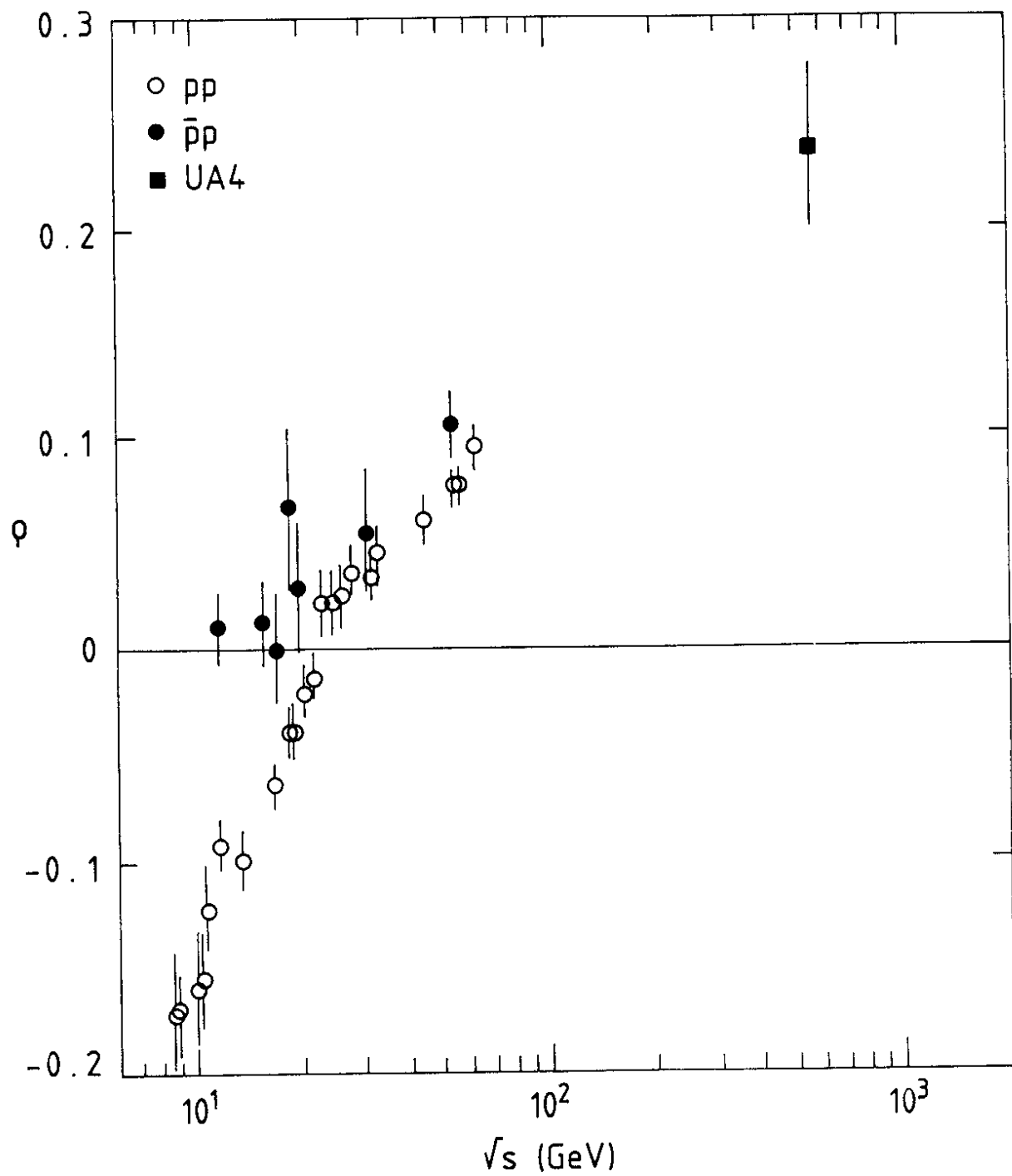


Fig. 4